Λ, Ξ and Ω production in Pb-Pb collisions at 158 A GeV/c

Presented by I. Králik for the WA97 collaboration:

E. Andersen[c], F. Antinori[e,k], N. Armenise[b], J. Bán[g], D. Barberis[f], H. Beker[e], W. Beusch[e], I.G. Bloodworth[d], J. Böhm[m], R.Caliandro[b], M. Campbell[e], E. Cantatore[e], N. Carrer[k], M.G. Catanesi[b], E. Chesi[e], M. Dameri[f], G. Darbo[f], A. Diaczek[l], D. Di Bari[b], S. Di Liberto[n], A. Di Mauro[b], D. Elia[b], D. Evans[d], K. Fanebust[c], R.A. Fini[b], J.C. Fontaine[i], J. Ftáčnik[g], B. Ghidini[b], G. Grella[o], M. Guida[o], E.H.M. Heijne[e], H. Helstrup[c], A.K. Holme[e], D. Huss[i], A. Jacholkowski[b], G.T. Jones[d], P. Jovanovic[d], A. Jusko[g], V.A. Kachanov[p], T. Kachelhoffer[q], J.B. Kinson[d], A. Kirk[d], W. Klempt[e], K. Knudson[e], I. Králik[e], J.C. Lassalle[e†], V. Lenti[b], R. Lietava[g], R.A. Loconsole[b], G. Løvhøiden[j], M. Lupták[g], V. Mack[i], V. Manzari[b], P. Martinengo[e], M.A. Mazzoni[n], F. Meddi[n], A. Michalon[q], M.E. Michalon-Mentzer[q], P. Middelkamp[e], M. Morando[k], M.T. Muciaccia[b], E. Nappi[b], F. Navach[b], P.I. Norman[d], B. Osculati[f], B. Pastirčák[g], F. Pellegrini[k], K. Píška[m], F. Posa[b], E. Quercigh[e], R.A. Ricci[h], G. Romano[o], G. Rosa[o], L. Rossi[f], H. Rotscheidt[e], K. Šafařík[e], S. Saladino[b], C. Salvo[f], L. Šándor[e,g], T. Scognetti[b], G. Segato[k], M. Sené[l], R. Sené[l], S. Simone[b], A. Singovski[p], W. Snoeys[e], P. Staroba[m], S. Szafran[l], M. Thompson[d], T.F. Thorsteinsen[c], G. Tomasicchio[b], T.S. Tveter[c], J. Urbán[g], G. Vassiliadis[a†], M. Venables[d], O. Villalobos Baillie[d], T. Virgili[o], A. Volte[l], M.F. Votruba[d] and P. Závada[m].

[a] Nuclear Physics Department, Athens University, Athens, Greece
[b] Dipartimento di Fisica dell'Università and Sezione INFN, Bari, Italy
[c] Fysisk institutt, Universitetet i Bergen, Bergen, Norway
[d] University of Birmingham, Birmingham, UK
[e] CERN, European Laboratory for Particle Physics, Geneva, Switzerland
[f] Dipartimento di Fisica dell'Università and Sezione INFN, Genoa, Italy
[g] Institute of Experimental Physics, Košice, Slovakia
[h] INFN, Laboratori Nazionali di Legnaro, Legnaro, Italy
[i] GRPHE, Université de Haute Alsace, Mulhouse, France
[j] Fysisk institutt, Universitetet i Oslo, Oslo, Norway
[k] Dipartimento di Fisica dell'Università and Sezione INFN, Padua, Italy
[l] Collège de France and IN2P3, Paris, France
[m] Institute of Physics, Czech Academy of Sciences, Prague, Czech Republic
[n] Dipartimento di Fisica dell'Università "La Sapienza" and Sezione INFN, Rome, Italy
[o] Dipartimento di Fisica dell'Università and INFN, Salerno, Italy
[p] Institute of High Energy Physics, Protvino, Russia
[q] Centre de Recherches Nucléaires, Strasbourg, France
† Deceased

Enhanced production of strange baryons and anti-baryons at central rapidity in S-W and S-S with respect to p-A reactions has been reported by the CERN experiments WA85 and WA94. The WA97 experiment is extending such a study to Pb-Pb collisions making use of the newly developed silicon pixel detectors.

Results on Λ, Ξ^- and Ω^- production in Pb-Pb collisions at 158 A GeV/c at central rapidity are presented. Transverse mass spectra and particle ratios are presented. Hyperon yields are given as a function of the collision centrality and compared with those obtained from p-Pb collisions using the same experimental setup.

1. INTRODUCTION

The study of relativistic heavy ion collisions provides a unique opportunity to search for a new predicted state of matter - the quark-gluon plasma (QGP). A number of experimental signatures which could signal the QGP have been proposed (see e.g. [1]). They are being studied in a number of experiments at the AGS and CERN SPS, however an unambiguous confirmation of the QGP formation has not yet been achieved.

Strange particles produced in heavy ion collisions give important information on the collision mechanism. In particular, the enhanced relative yield of strange and multi-strange particles in nucleus-nucleus reactions with respect to hadronic interactions has been suggested as one of the sensitive signatures for a phase transition to a QGP state [2,3]. It is expected that the enhancement should be more pronounced for multi-strange than for singly strange particles [4].

In the QGP scenario the strangeness enhancement could be created as a result of rapidly developing flavour equilibration. Strange quark pairs are easily produced in a gluon rich QGP environment, predominantly in gluon-gluon interactions. The equilibration time is estimated to be comparable with the interaction time of the high energy heavy-ion collision (a few fm/c).

Strangeness production can also be enhanced in a purely hadronic scenario (hot and dense hadronic gas), where the relative abundance of strange particles could grow gradually in a chain of rescattering processes. The characteristic time scale in this case is estimated to be much longer, of the order of 100 fm/c.

Three heavy ion experiments dedicated to the study of strangeness production were performed at the Omega spectrometer: WA85, WA94 and WA97.

The WA85 and WA94 experiments utilised the 200 A GeV/c SPS sulphur beam. WA85 investigated strangeness production in p-W and S-W collisions, while WA94 studied p-S and symmetric S-S interactions. Both experiments used a tracking system with multiwire proportional chambers modified to be sensitive only to a few particles emitted at central rapidity and $p_\perp > 1$ GeV/c. Particle ratios measured by both experiments showed evidence for enhanced production of strange and multi-strange particles in nucleus-nucleus with respect to proton-nucleus collisions [5,6].

The encouraging results from WA85 and WA94 on strangeness production lead naturally to a question of how this picture will evolve when a truly heavy ion beam (Pb) is used. Answering this question is a task of the WA97 experiment.

2. EXPERIMENT WA97

2.1. Experimental set-up

The WA97 set-up, shown schematically in Fig. 1, is described in detail in ref. [7]. The target and the silicon telescope were placed inside the homogeneous 1.8 T magnetic field of the CERN Omega magnet.

158 A GeV/c lead beam from the CERN SPS was impinging on a lead target with thickness corresponding to 1% of the interaction length. Scintillator petal detectors behind the target provided an interaction trigger selecting roughly 30% of the most central Pb-Pb collisions. Two planes of microstrip multiplicity detectors covering the pseudorapidity region $2 < \eta < 4$ provided information for more detailed off-line study of the centrality dependence of particle ratios and spectra.

The heart of the WA97 spectrometer was the silicon telescope consisting of 7 planes of silicon pixel detectors with a pixel size 75×500 μm, and of 10 planes of silicon microstrips with a 50 μm pitch. The telescope has $5{\times}5$ cm^2 cross section and contained $\approx 0.5{\times}10^6$ channels. This tracking device was placed 60 cm behind the target (90 cm for the p-Pb reference run) slightly above the beam line and inclined (pointing to the target) in order to accept particles at central rapidity and medium transverse momentum.

The track recognition was done in the compact part of the silicon telescope (30 cm long, with 6 pixel and 5 microstrip planes). The momentum resolution of fast track was improved using the lever arm detectors (1 pixel and 5 microstrip planes) and three MWPC's with a cathode pad readout placed outside the magnet.

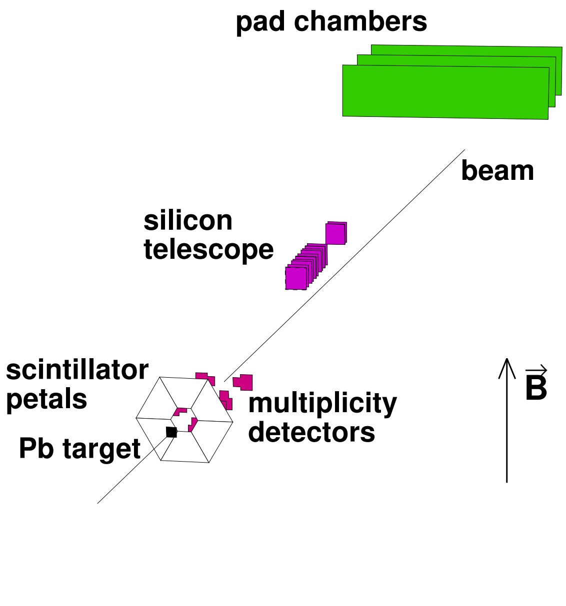

Figure 1. The WA97 set-up.

2.2. Data samples and selection criteria

The results presented here are based on the analysis of two data samples taken during the 1995 run with proton (120 million events) and lead beams (110 million events) at 158 A GeV/c.

Λ, Ξ^-, Ω^- and their antiparticles were identified by reconstructing their decays into final states containing only charged particles:

$$\begin{array}{lll} \Lambda & \rightarrow & \mathrm{p}+\pi^- \\ \Xi^- & \rightarrow & \Lambda+\pi^- \\ & & \hookrightarrow \mathrm{p}+\pi^- \\ \Omega^- & \rightarrow & \Lambda+\mathrm{K}^- \\ & & \hookrightarrow \mathrm{p}+\pi^- \end{array}$$

The Λ decay vertex was required to fall within a fiducial region starting at 30 cm or 40 cm from the target for Pb-Pb and p-Pb runs, respectively. The fiducial region for Ξ and Ω [1] decays started at 20 cm after the target. At both the Λ and cascade (Ξ, Ω) decay vertices a distance of closest approach between trajectories of decay particles of less than 1 mm was required. A standard set of cuts analogous to those described in [5] was applied to eliminate the background. The Λ candidates were required to be kinematically

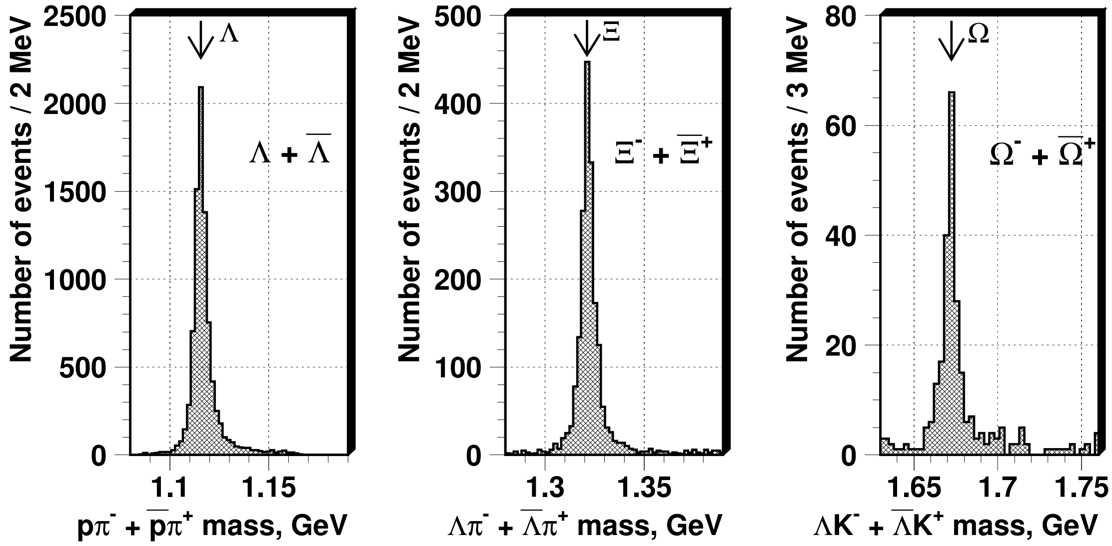

Figure 2. Hyperon signals and mass resolution in Pb-Pb data.

unambiguous with the $\mathrm{K}^0_{\mathrm{s}}$, and the Ω candidates with Ξ decays. Λ, Ξ and Ω candidates were required to point back to the primary vertex. The quality of the data can be judged

[1]In the following, symbols Λ, Ξ and Ω refer to both hyperons and their antiparticles.

from the plots in Fig. 2. Precise knowledge of the primary vertex position was essential for efficient background elimination from Ξ and Ω mass spectra.

The hyperon data had to be corrected for geometrical acceptance and reconstruction efficiency. Weights for each reconstructed Λ, Ξ and Ω were calculated by a GEANT based Monte Carlo procedure on event-by-event basis. For each particle a large sample of hyperon decays with the same (measured) rapidity, $p_\perp$ and position of the primary vertex was generated. The tracks of the decay products were traced through the WA97 set-up. The detection efficiencies for each read-out chip of the pixel and microstrip planes have been determined and taken into account.

Background tracks and electronic noise were simulated by embedding the hits from the simulated events into real events with hit multiplicity close to that of the original event. These mixed events were processed in the same way as the real ones (pattern recognition, track fitting, hyperon selection). The resulting weight was calculated as the number of Monte Carlo events generated divided by the number of Monte Carlo events successfully reconstructed.

Up to now only a fraction of the full available data sample was fully corrected. Table 1 shows the hyperon samples used for the present analysis as well as the expected increase in statistics after processing and correcting all collected data.

Table 1
Hyperon statistics used in the present analysis and expected increase in the statistics after processing all available data.

	Pb-Pb		p-Pb	
Particle	QM'97	Expected increase	QM'97	Expected increase
Ω^-	77	$\times 5$	15	-
$\overline{\Omega}^+$	30	$\times 5$	4	-
Ξ^-	715	$\times 5$	275	-
$\overline{\Xi}^+$	187	$\times 5$	101	-
Λ	447	$\times 1500$	515	$\times 200$
$\overline{\Lambda}$	301	$\times 300$	126	$\times 200$

The acceptance windows for Λ, Ξ and Ω from Pb-Pb collisions is shown in Fig. 3 and 4. For p-Pb data, the windows are a bit different because the silicon telescope was placed further away from the target.

For Pb-Pb collision, the symmetry of the system around midrapidity (in our case $y_{cm} = 2.91$) allows us to obtain information on hyperon production within one unit of rapidity around y_{cm}. To obtain particle ratios and yields in a well defined kinematic region we extrapolated the data in the following way:

- $d^2N/dm_\perp dy$ of hyperons were fitted in the corresponding acceptance windows using the log likelihood method, and

- the particle yields were extrapolated to a region $|y - y_{cm}| < 0.5$ and $p_\perp \geq 0.7$ GeV/c

or $p_\perp \geq 0$ GeV/c.

For the present analysis we assumed the rapidity distributions to be flat for $|y - y_{cm}| < 0.5$.

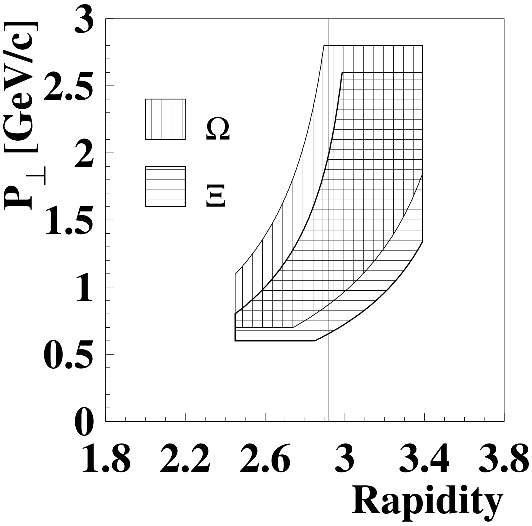

Figure 3. Acceptance windows for Ξ and Ω in Pb-Pb sample.

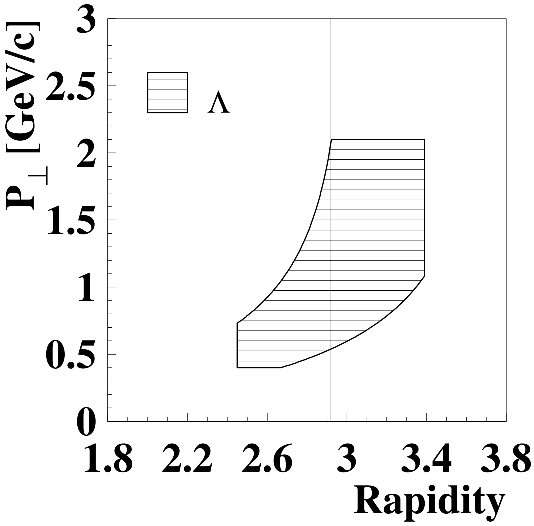

Figure 4. Acceptance window for Λ in Pb-Pb sample.

3. RESULTS

3.1. Measurement of $dN/d\eta$

The charged particle multiplicity in the pseudorapidity window $2 < \eta < 4$ was measured during a special Pb-Pb run without magnetic field. The raw information from the microstrip multiplicity detectors was corrected for geometrical acceptance, secondary interactions and delta rays. The results, corresponding to the most central 30% of the inelastic Pb-Pb collisions are shown in Fig. 5. The small irregularities visible in the $dN/d\eta$ distribution suggest some remaining systematic problems to be removed by further analysis of multiplicity data.

3.2. Transverse mass spectra of Λ, Ξ and Ω

The transverse mass spectra for Λ, Ξ and Ω have been parametrised by

$$\frac{dN}{dm_\perp} \propto m_\perp^\alpha \exp(-\frac{m_\perp}{T}). \tag{1}$$

For better comparison with various theoretical models we used two different values of α:

- $\alpha = 1$: expected when particles emitted by a single stationary fireball have been collected in a narrow rapidity window, and

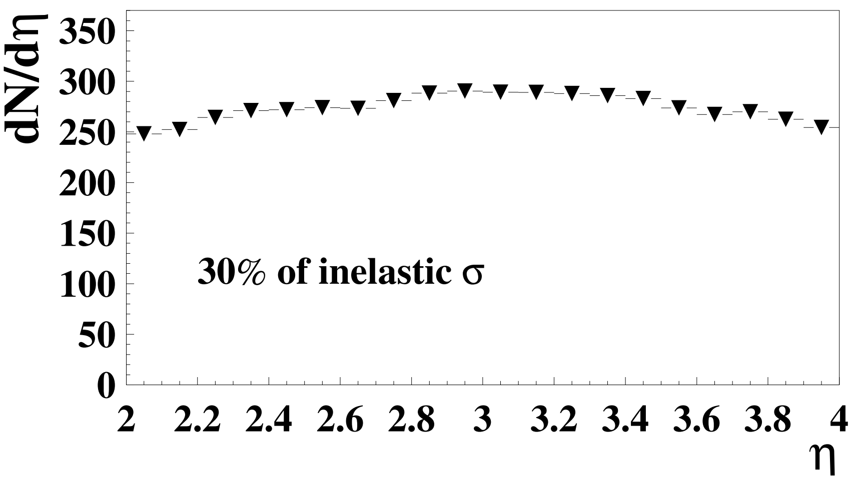

Figure 5. $dN/d\eta$ distribution for 30% of the total inelastic Pb-Pb cross section.

- $\alpha = 3/2$: expected when particles emitted by a single stationary fireball have been collected in a wide rapidity window or when particles emitted by many fireballs moving relative to each other with a boost-invariant longitudinal velocity profile, have been collected in a narrow rapidity window. For details see [8].

As an example, the Ξ^- and $\overline{\Xi}^+$ spectra with the corresponding fits are shown in fig. 6. The inverse slope parameters T for Λ, Ξ and Ω measured in Pb-Pb and p-Pb collisions are summarised in Table 2. Due to small statistics (see Table 1), data on Ω^- and $\overline{\Omega}^+$ in Pb-Pb were put together. For p-Pb data the statistics (19 Ω) were not enough to estimate T.

An analysis [9] of the T parameters of $\pi^\pm$, $\mathrm{K}^\pm$, K^0_s, p, $\overline{\mathrm{p}}$, Λ, $\overline{\Lambda}$ and deuteron measured in Pb-Pb collisions [10] indicates a linear increase of T with particle mass which can be interpreted as an indication of transverse flow. Fig. 7 shows the results already published by the NA49 collaboration [10] together with our results on hyperons. One can see that while T increases steadily with mass from π to p, for Λ, Ξ and Ω one observes a flattening of such a T dependence on mass. The reason of such a flattening have to be understood.

3.3. Particle ratios and yields

Particle ratios involving Λ, Ξ^-, Ω^- and antiparticles in Pb-Pb collisions are shown in Table 3 for two different kinematic windows (one unit of rapidity around y_{cm} and $p_\perp \geq 0.7$ GeV/c or $p_\perp \geq 0$ GeV/c).

The WA97 trigger selects the 30% most central Pb-Pb collisions and we measure the charged particle multiplicity in $2 < \eta < 4$ interval. From this multiplicity we estimate the centrality of the collisions e.g. the number of participants and the number of binary nucleon-nucleon collisions $\langle n_{collisions} \rangle$ using a geometric model for Pb-Pb interactions. For

Table 2
Inverse $m_\perp$ slope parameters in MeV for two different values of exponent in the parametrization function (see text for details).

Particle	Pb-Pb		p-Pb	
	$\alpha = 3/2$	$\alpha = 1$	$\alpha = 3/2$	$\alpha = 1$
Λ	267 ± 15	291 ± 18	191 ± 8	203 ± 9
$\overline{\Lambda}$	257 ± 17	280 ± 20	170 ± 14	180 ± 15
Ξ^-	269 ± 11	289 ± 12	222 ± 12	235 ± 14
$\overline{\Xi}^+$	251 ± 19	269 ± 22	211 ± 19	224 ± 21
$\Omega^- + \overline{\Omega}^+$	225 ± 22	237 ± 24	-	-

Table 3
Comparison of particle ratios measured in Pb-Pb collisions. Lower $p_\perp$ cut values are given in GeV/c.

Ratio	Pb-Pb	
	$p_\perp > 0.7$	$p_\perp > 0$
$\overline{\Lambda}/\Lambda$	0.124 ± 0.013	0.128 ± 0.012
$\overline{\Xi}^+/\Xi^-$	0.255 ± 0.025	0.266 ± 0.028
$\overline{\Omega}^+/\Omega^-$	0.38 ± 0.10	0.46 ± 0.15
Ξ^-/Λ	0.099 ± 0.008	0.093 ± 0.007
$\overline{\Xi}^+/\overline{\Lambda}$	0.203 ± 0.024	0.195 ± 0.023
Ω/Ξ	0.192 ± 0.024	0.195 ± 0.028

p-Pb interaction, the estimated $\langle n_{collisions} \rangle$ corresponds to minimum bias collisions.

Fig. 8 shows the Λ, Ξ and Ω yields as a function of $\langle n_{collisions} \rangle$. Yields are calculated in the window $|y - ycm| < 0.5$ and $p_\perp \geq 0.7$ GeV/c. All hyperon yields show a steady increase with centrality up to very central events.

Fig. 9 shows the hyperon yields per binary collision expressed in units of corresponding yield per collision in p-Pb reaction (i.e. each yield per collision is rescaled so that each value for p-Pb is set to one) as a function of $\langle n_{collisions} \rangle$. One can see that Λ, Ξ and Ω yields increase with centrality faster than number of collisions. Moreover, this increase is larger for Ω than for Ξ, which in turn increases more than Λ.

4. CONCLUSIONS AND OUTLOOK

The results that we consider most significative concern the inverse slopes T and the increase of hyperon yields versus the number of collisions.

T is found to be lower for Ω than for Λ and Ξ and a clear deviation from the linear dependence of T on particle mass (discussed in [9] as an evidence of radial flow in nucleus-nucleus collisions) is observed.

The hyperon yields increase from p-Pb to central Pb-Pb faster than the estimated

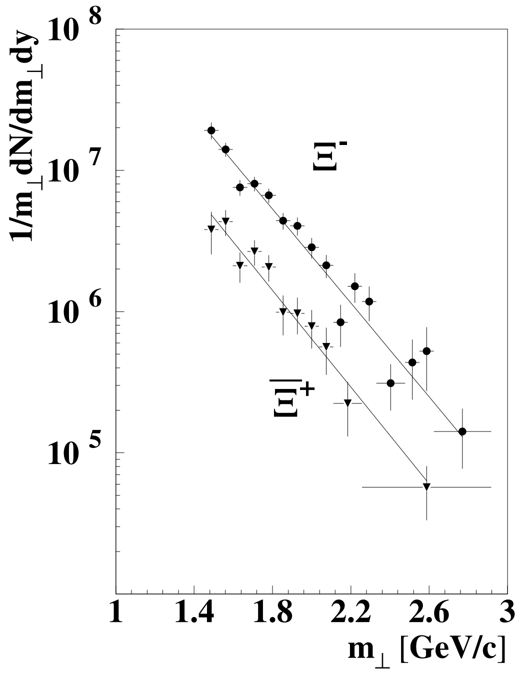

Figure 6. $m_\perp$ spectra of Ξ^- and $\overline{\Xi}^+$ with the results of fit superimposed.

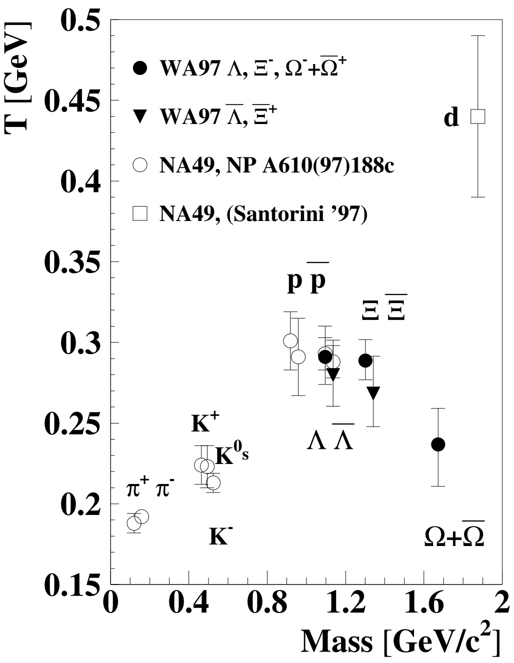

Figure 7. Inverse $m_\perp$ slope parameter T dependence on the particle mass.

number of binary nucleon-nucleon collisions (by an order of magnitude in the case of the Ω). The data show no sign of saturation of hyperon production with increasing centrality of Pb-Pb collisions.

The observed strangeness enhancement exhibits an $\Omega > \Xi > \Lambda$ hierarchy, i.e. the Ω yield grows faster with centrality than that of the Ξ, and the Ξ yield faster than that for the Λ.

Further extensions of the analysis presented are in progress. The WA97 collaborations aims:

(i) to study with large statistics (adding also the p-Be point) the behaviour of yields as a function of the number of collisions and the number of participants, and

(ii) to complete the above study with data on K^0_s and negative hadrons.

REFERENCES

1. J.W. Harris and B. Müller, Annu. Rev. Nucl. Part. Sci. 46 (1996) 71.
2. J. Rafelski and B. Müller, Phys. Rev. Lett. 48 (1982) 1066
   J. Rafelski and B. Müller, Phys. Rev. Lett. 56 (1986) 2334.
3. P. Koch, B. Müller and J. Rafelski, Phys. Rep. 142 (1986) 167.

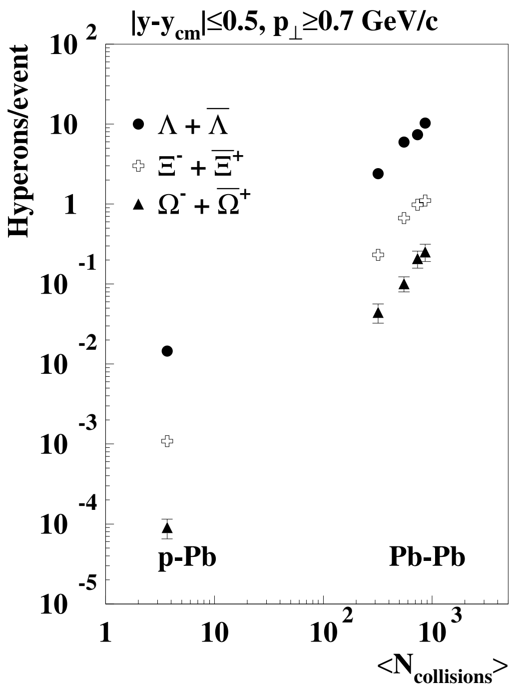

Figure 8. Λ, Ξ and Ω yields as a function of the mean number of inelastic nucleon-nucleon collisions (see text for details).

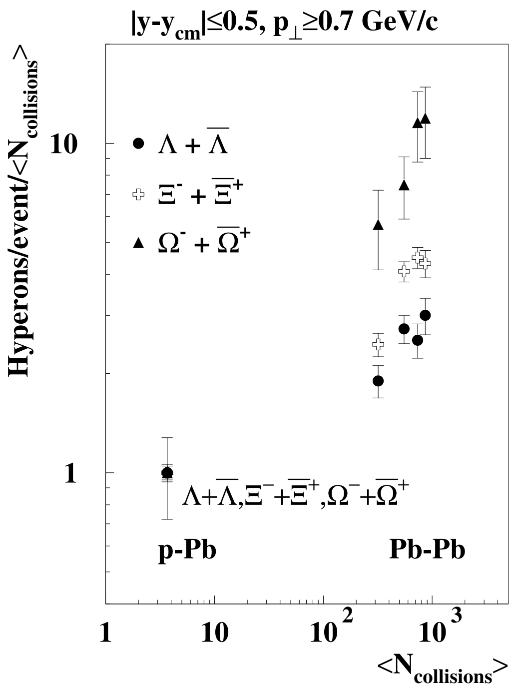

Figure 9. Λ, Ξ and Ω yields per inelastic collisions expressed in units of yield per collision observed in p-Pb data.

4. J. Rafelski, Phys. Lett. B262 (1991) 333.
5. S. Abatzis et al., Nucl. Phys. A590 (1991) 307c,
   S. Abatzis et al., Phys. Lett. B400 (1997) 223.
6. S. Abatzis et. al., Nucl. Phys. A590 (1995) 317c.
7. G. Alexeev et al., Nucl. Phys. A590 (1995) 139c.
8. E. Schnedermannn, J. Sollfrank and U. Heinz, NATO ASI Series B303 (1993) 175.
9. B. Kämpfer, preprint FZR-149, September 1996, hep-ph/9612336.
10. P.G. Jones et. al (NA49 Collaboration), Nucl. Phys. A610 (1996) 188c.
11. A. Bamberger et al., Z. Phys. C43 (1989) 25.